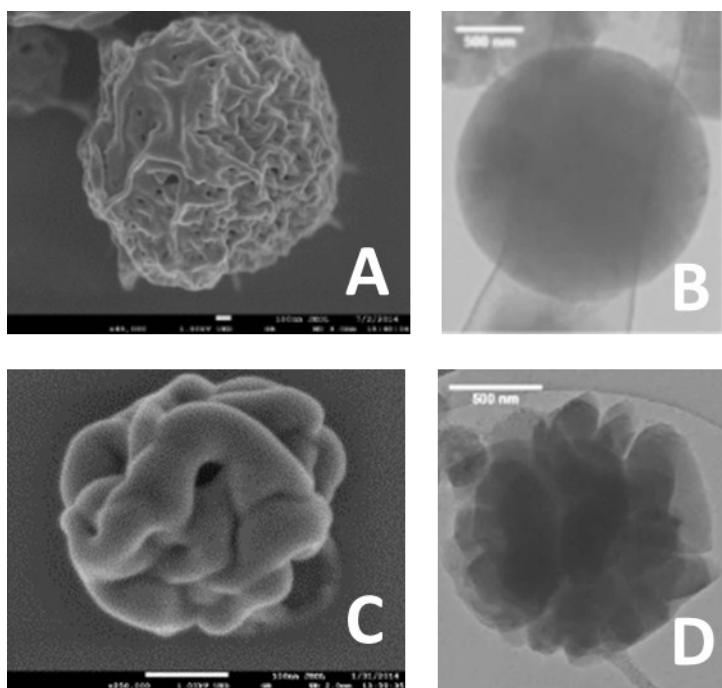
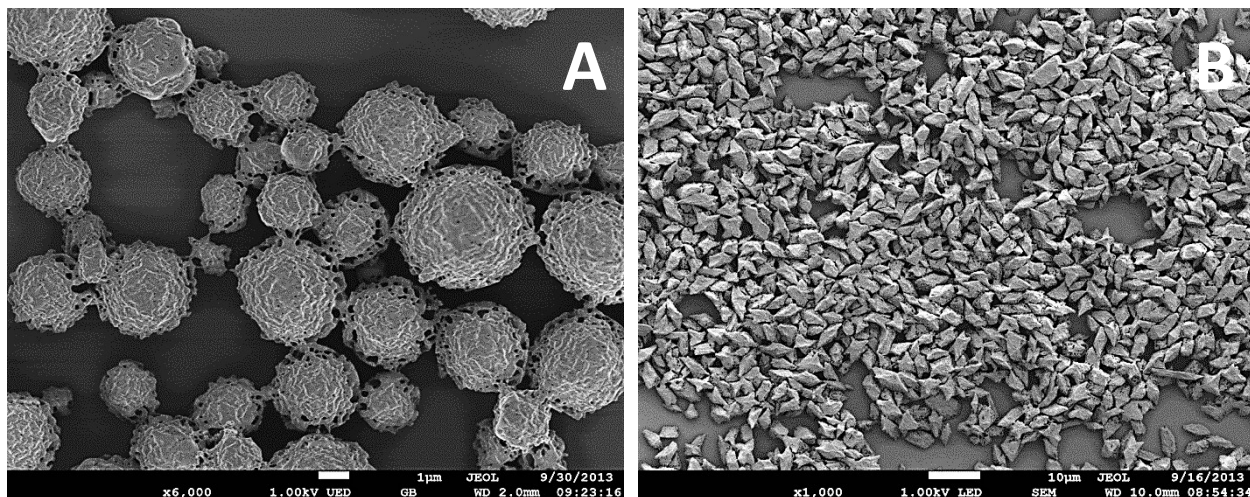


**Fig. S1.** The reaction generating the sulfur particles evolves  $\text{SO}_2$  gas which often results in hollow domains of the sulfur core and the partial rupturing of the initial polymer coating. SEM imaging shows the hollow domains of the sulfur core as well as the ruptured polymer coating (panels A and B). Depending on the  $T_g$  of the polymers used, the initial polymer coating retains the spherical shape even after all the sulfur contents were sublimed in the oven (panel C). It is important to note that the optimized truffle cathode contains 7 additional polymer layers which encapsulate the ruptured particles well.



**Fig. S2.** SEM (A and C) and TEM (B and D) of sulfur particles stabilized by an “embryonic” membrane which do not contain conductive carbon embedded inside the sulfur core ((A and B) and which contain embedded carbon (C and D). Notice the presence of carbon inside the sulfur particle core changes the surface morphology creating deep invaginations (C). TEM imaging also shows dense heterogeneous areas inside the sulfur particle which presumably corresponds to the presence of embedded carbon (C).



**Fig. S3.** Two distinct shapes of sulfur particles obtained in situ by the reaction described in the manuscript with the same polymer. A dilute solution of PEDOT:PSS yields the spherical particles in panel A while a mixture 10 times more concentrated yields the rhomboidal particles in panel B.

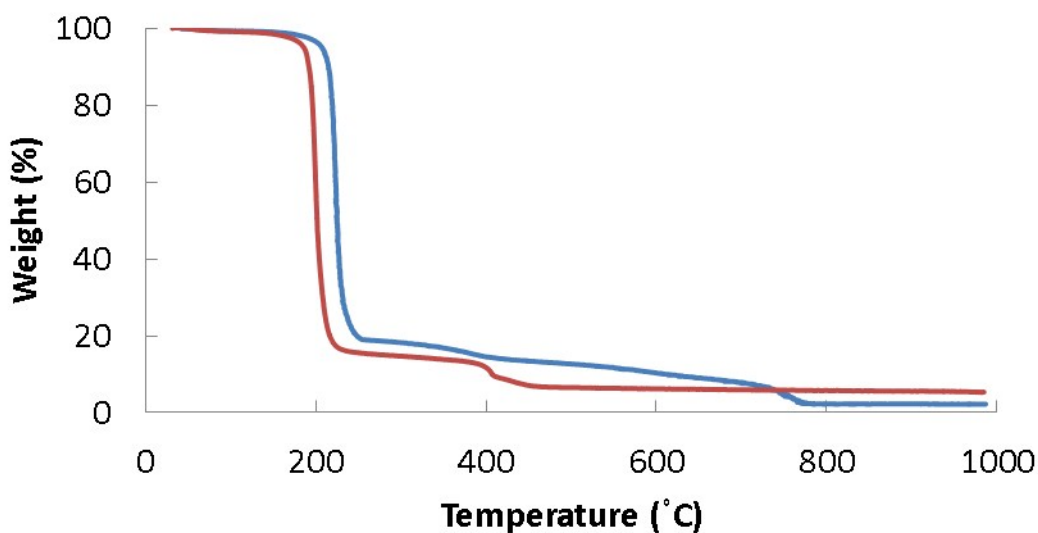


**Fig. S4.** TGA of the active material with a mature membrane composed of 7 layers (PEDOT:PSS/PDADMA) in garnet color with approximately 85% sulfur content and the active material wrapped in a mature membrane composed of 7 layers (PVP/PAA/PEO) in blue color with 82% sulfur content.

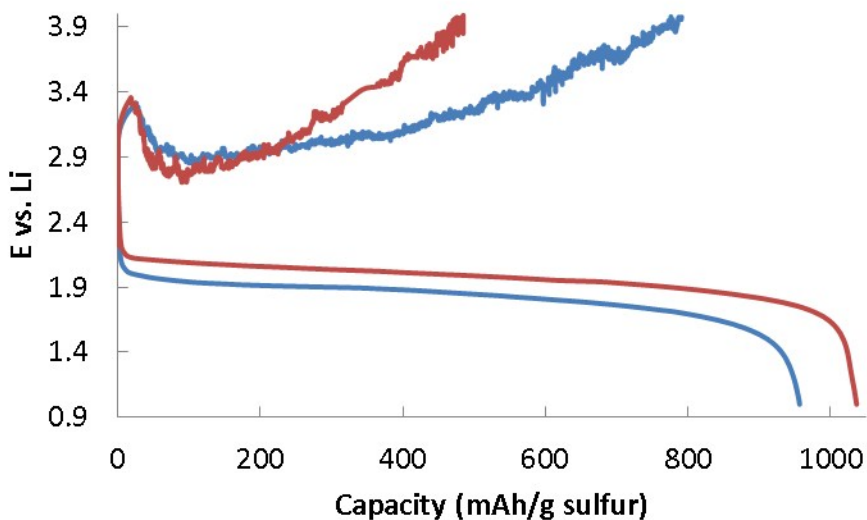


**Fig. S5.** A higher capacity is observed when 5% hexane is added (by volume) to the electrolyte mixture (garnet line). Discharge with a “base” electrolyte without hexane is shown in blue. The “base” electrolyte was composed of 1.0M LiBOB in dioxolane:glyme in a 1:1 mixture. The cathode was a non-optimized sulfur cathode. Batteries consist of 2032 coin cells with a sulfur loading of  $\sim 1 \text{ mg/cm}^2$  and  $\sim 50\%$  sulfur loading by mass in the finished cathode. Cycling was performed at a fast rate of 2C.

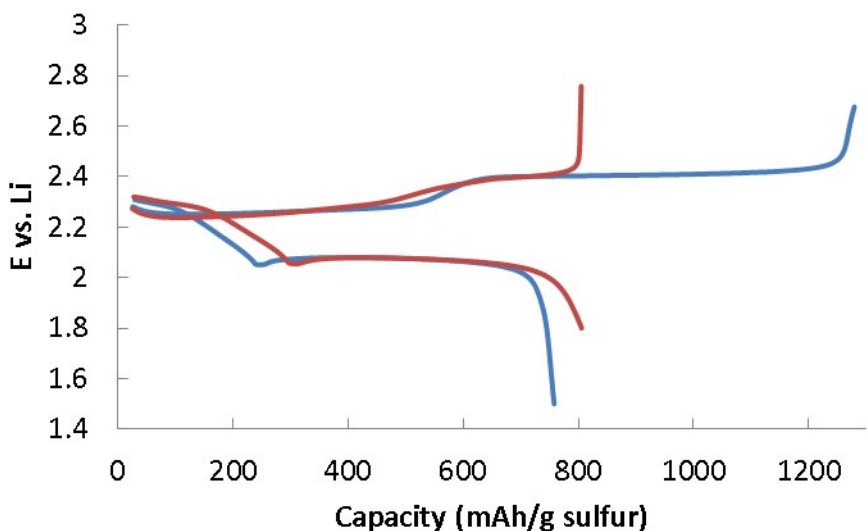


**Fig. S6.** No overcharge and a higher capacity is observed when the “base” electrolyte mixture contains lithium polysulfides (5M) (garnet line). Discharge with a “base” electrolyte without lithium polysulfides is shown in blue. The “base” electrolyte was composed of 1.0M LiTFSI dissolved in dioxolane:glyme in a 1:1 mixture. The cathode was a non-optimized sulfur cathode. Batteries consist of 2032 coin cells with a sulfur loading of  $\sim 1 \text{ mg/cm}^2$  and  $\sim 50\%$  sulfur loading by mass in the finished cathode. Cycling was performed at a rate of 0.5C.

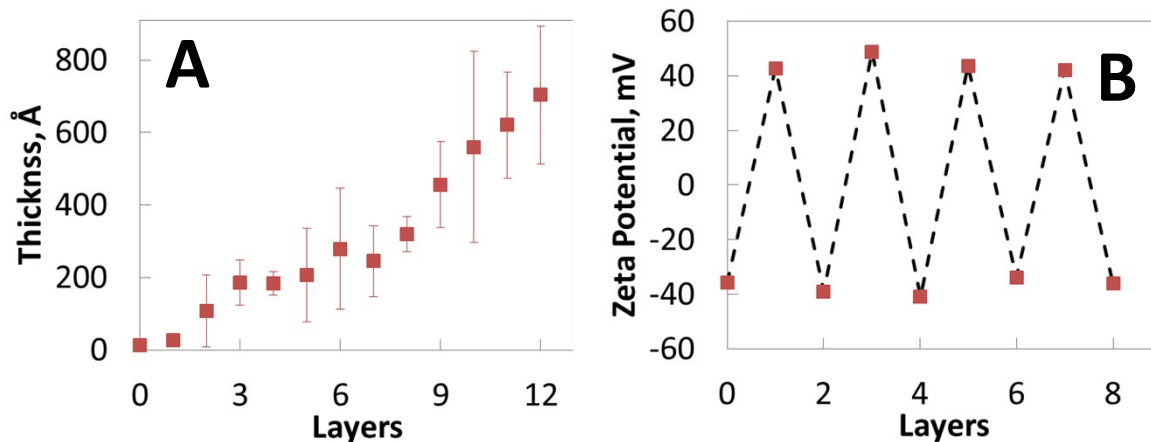


**Fig. S7.** A) Layer by layer adsorption of multilayer nanomembranes composed of PPy/PEDOT:PSS on flat, polished silicon wafer surrogate substrates from dilute polymer solutions as described in the experimental section. The thickness of each (nitrogen gas) dried layer was measured with a Gaertner ellipsometer. Once assembled from aqueous solutions, the film experiences no significant change in thickness after dipping overnight in battery electrolyte solvents.; B) zeta potential measurement of surface charge alternation due to LBL nanomembrane adsorption on the sulfur particle as tabulated below.

Layer #	Layer Composition	Zeta potential (mV)
0	embryonic layer (PEDOT:PSS)	-35.9
1	PDAD	+42.7
2	PEDOT:PSS	-39.1
3	PDAD	+48.8
4	PEDOT:PSS	-41.2
5	PDAD	+43.7
6	PEDOT:PSS	-33.9
7	PDAD	+42.1
8	functionalized carbon	-36.1

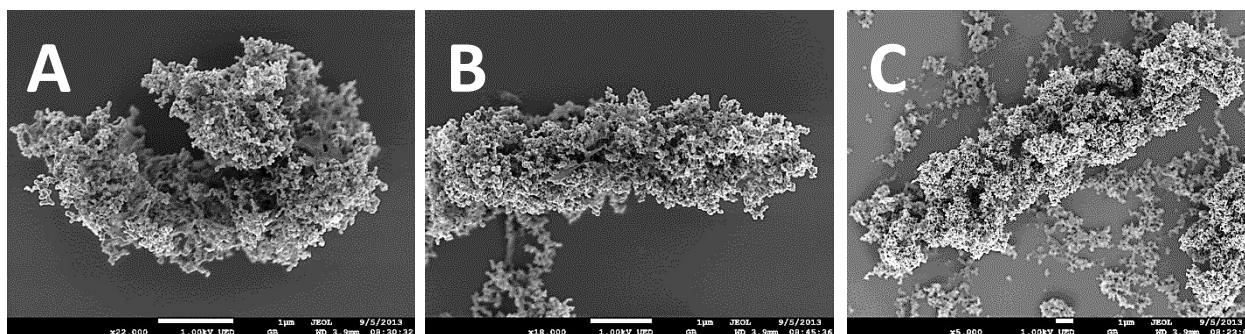


**Fig. S8.** Excess carbon decoration on polymer coated sulfur particles.

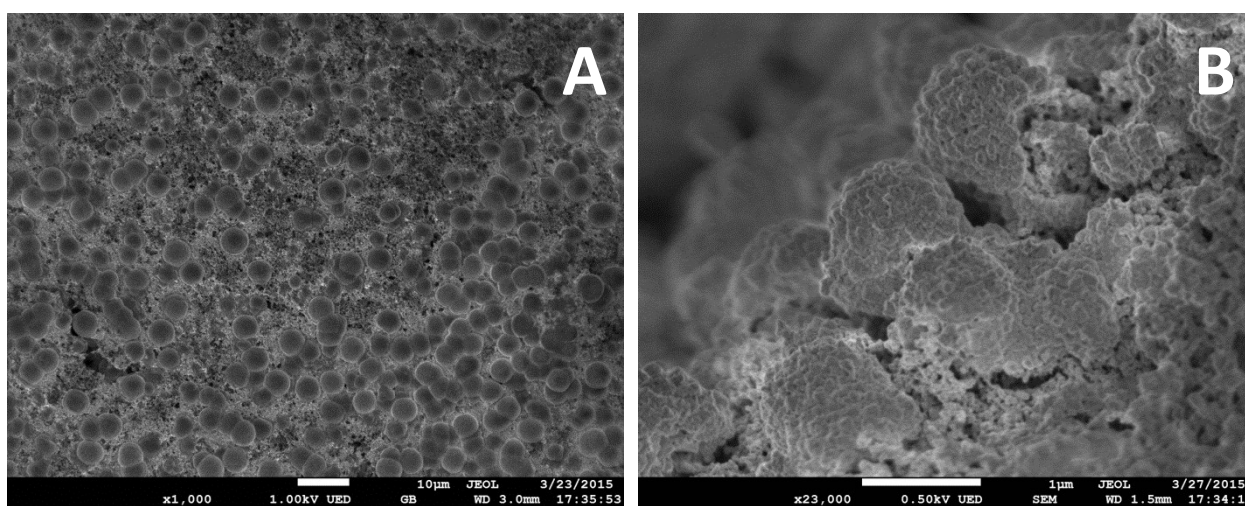


**Fig.S9.** SEM images of non-optimized sulfur particles mixed in a preliminary cathode after battery cycling. A) shows a carbon-free variant of the sulfur particles while B) shows a carbon coated variant. The generally spherical shape of the particles is maintained after battery cycling presumably due to the polymer membrane limiting the loss of active material.

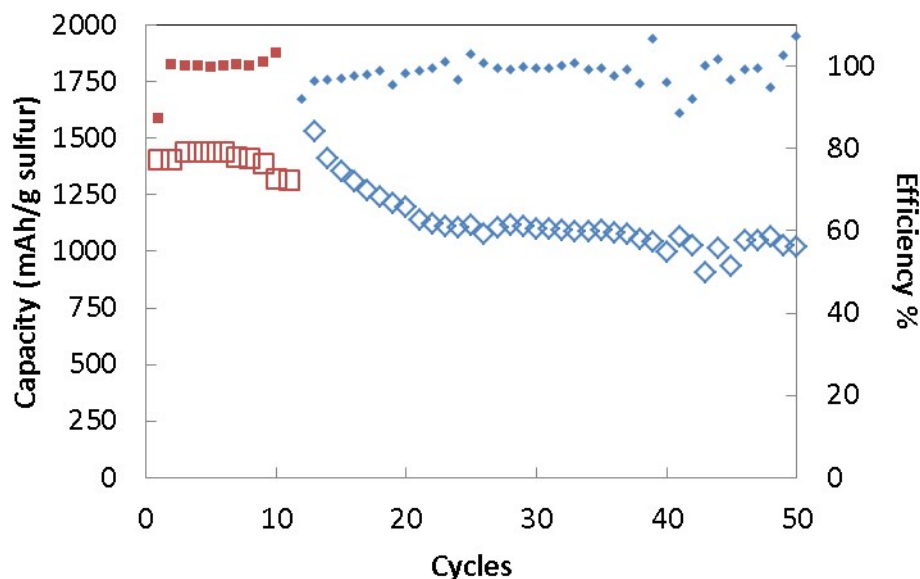


**Fig. S10.** Battery operation for optimized truffle cathodes at a slow rate of 0.5C. Cycling was interrupted for 2 days after cycle 11 and then resumed. No self-discharge is observed during the pause and the battery starts discharging at a slightly higher capacity after the break. Batteries consist of 2032 coin cells with a sulfur loading of  $\sim 1 \text{ mg/cm}^2$  and  $\sim 50\%$  sulfur loading by mass in the finished cathode.

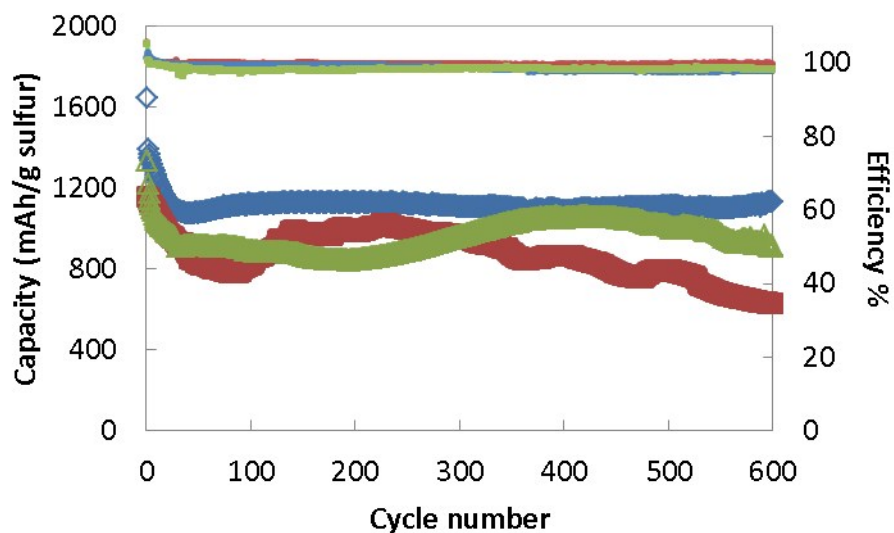


**Fig. S11.** Capacity fade over the first 600 cycles for optimized truffle cathodes (7 layers PVP/PAA/PEO). Batteries consist of 2032 coin cells with a sulfur loading of  $\sim 1 \text{ mg/cm}^2$  and  $\sim 50\%$  sulfur loading by mass in the finished cathode. Battery cycling was performed at 0.5C (green), 2C (blue) and 5C (garnet).